



Aalborg Universitet

AALBORG UNIVERSITY
DENMARK

Harmonics Mitigation in Cascaded Multilevel PV Inverters During Power Imbalance Between Cells

Lashab, Abderezak; Séra, Dezso; Guerrero, Josep M.

Published in:

Proceedings - 2019 IEEE International Conference on Environment and Electrical Engineering and 2019 IEEE Industrial and Commercial Power Systems Europe, IEEEIC/I and CPS Europe 2019

DOI (link to publication from Publisher):

[10.1109/IEEEIC.2019.8783901](https://doi.org/10.1109/IEEEIC.2019.8783901)

Publication date:

2019

Document Version

Accepted author manuscript, peer reviewed version

[Link to publication from Aalborg University](#)

Citation for published version (APA):

Lashab, A., Séra, D., & Guerrero, J. M. (2019). Harmonics Mitigation in Cascaded Multilevel PV Inverters During Power Imbalance Between Cells. In *Proceedings - 2019 IEEE International Conference on Environment and Electrical Engineering and 2019 IEEE Industrial and Commercial Power Systems Europe, IEEEIC/I and CPS Europe 2019* [8783901] IEEE Press. <https://doi.org/10.1109/IEEEIC.2019.8783901>

General rights

Copyright and moral rights for the publications made accessible in the public portal are retained by the authors and/or other copyright owners and it is a condition of accessing publications that users recognise and abide by the legal requirements associated with these rights.

- ? Users may download and print one copy of any publication from the public portal for the purpose of private study or research.
- ? You may not further distribute the material or use it for any profit-making activity or commercial gain
- ? You may freely distribute the URL identifying the publication in the public portal ?

Take down policy

If you believe that this document breaches copyright please contact us at vbn@aub.aau.dk providing details, and we will remove access to the work immediately and investigate your claim.

Harmonics Mitigation in Cascaded Multilevel PV Inverters During Power Imbalance Between Cells

Abderezak Lashab, Dezso Sera, Josep M. Guerrero

Department of Energy Technology, Aalborg University, Aalborg DK-9220, Denmark
abl@et.aau.dk, des@et.aau.dk, joz@et.aau.dk

Abstract—This paper presents a grid connected multilevel topology for photovoltaic (PV) systems. Usually, multilevel converters for PV application suffer from a distorted output current and voltage when the submodules are not subjected to an even solar irradiance. The difference in submodules irradiance results in different submodules duty cycles when maintaining the maximum power point tracking (MPPT). The distortion of the output current is proportional with the difference of the cells duty cycles. To this regard, a multilevel topology for PV applications is proposed along with a control and modulation strategy. In this proposed topology, H6 bridge-based cell is used instead of an H-bridge one. In case of solar irradiance mismatch, the proposed converter injects power with less voltage from the shaded cells without altering the PV voltage, and hence, the MPPT. This modification allows retaining a tantamount duty cycle in all cells whatever the meteorological conditions are present. To test the effectiveness of the proposed idea, a detailed simulation model was set up. The results show that the proposed concept provides a significantly improved output current quality compared to the cascaded H-bridge topology.

Keywords—Cascaded converter, Grid connected, H-bridge, MMC, MPPT, Partial shading, Photovoltaic, P&O, Power quality.

I. INTRODUCTION

The integration of renewable energy sources such as photovoltaics is continually increasing, which is motivating researchers to design high efficiency, reliable and low cost dc-ac inverters. Several PV inverter categories were tested in the last decades, and they can be grouped as centralized, string, multi-string, module integrated, and cascaded categories [1]. In Centralized category, an inverter is dedicated to the whole PV strings, which could be a voltage source converter, an H-bridge inverter, flying capacitor...etc [2]-[3]. Each PV string is feeding the grid through an inverter in string category [4]. In multi-string category, the inverter connected to the grid is fed by a paralleled dc-dc converters, which are connected to a PV string each [5]. Each module is connected to a small rating inverter (micro-inverter), in module integrated category [6]. Cascaded topology can be sub-divided into two main classes:

1-Cascaded dc-dc: in this class, each string is connected to a dc-dc converter, and these converters are cascaded to

form a dc-link for a high voltage inverter, the latter is usually a modular multilevel converter (MMC) [7].

2-Cascaded dc-ac: each string is connected to a dc-ac inverter, and these inverters are cascaded to form together the grid current [8].

Modular multilevel converters are a very promising candidate since they offer a robust, efficient, and fault tolerant power electronic converters [9]. These power converter topologies can provide high-quality voltage waveforms with semiconductor switches working at a frequency near the fundamental when the number of levels is high. Among them, the cascaded H-bridge (CHB) power converter [10], which is composed of a series connection of H-bridges, each one of them is connected to a separate dc voltage source. This feature allows the connection of PV panels in each H-bridge, and hence independent maximum power point tracking can be performed, which in its turn, increases the efficiency of the overall system and the energy injected to the grid [11]-[12].

The commonly used Pulse Width Modulation (PWM) technique in multilevel converters is the Phase Shifted PWM (PS-PWM) [13]. In CHB application, the PS-PWM is described as a unipolar multi-carriers, one carrier for each H-bridge, where the shift between these carriers is equal to π/n (n is the number of H-bridges). This modulation strategy offers equal power distribution and equal power losses among the H-bridges, as well as multiplicative effect ($2nm_f$) of the output voltage switching-frequency [13].

However, in case the H-bridges are subjected to uneven solar irradiance, due to partial shading or dust on the PV panels, high order harmonics are generated in the injected current to the grid. Several works that deal with this problem are reported in the literature [14]-[17]. In [14], the balance of the H-bridge voltages is considered by using Zero Sequence Generation approach; however, this strategy does not seem to be suitable for PV applications since the H-bridge voltage should be regulated by using an MPP tracker. In [15], the use of a variable shifting angle is the main principle, this approach offers a cheap solution, but, it is appropriate only when using three cascaded H-bridges. The authors in [16], proposed the use of an extra battery fed H-bridge to overcome this problem in case two cascaded H-bridges are used. The focus when the partial shading takes place between the phases, instead of within the cells of one phase was considered in [17].

The main cause of the harmonics generated in the output signals when the solar irradiance is not balanced, is the difference in the duty cycles. When the irradiance decreases,

The authors acknowledge the support of the Danish Energy Technology Development and Demonstration Program (EUDP) through the project PVST – PV+STorage Operation and Economics in distribution systems, project nr. 12,551.

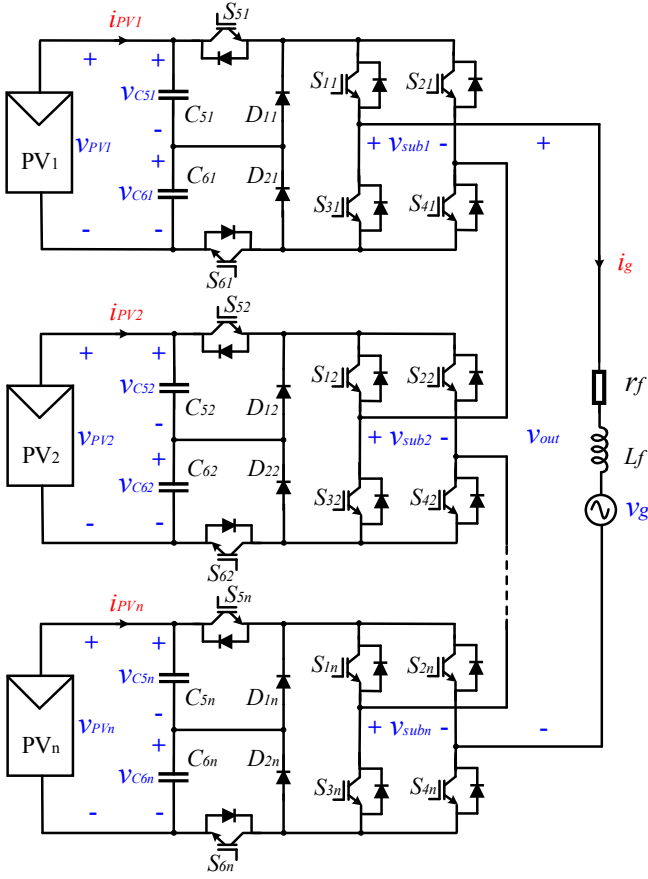


Fig. 1. The proposed cascaded multilevel topology for PV systems.

the controller limits the duty cycle in order for the shaded PV panel to match its new MPP current, consequently, different duty cycles are fed to the modulator. In this case, the shaded cell starts injecting power with a certain delay (t_d) and stops injecting power before the expected time by a t_d . Since in modular multilevel converters the cells are grouped together to form the output signal (output current and voltage), the timing is a critical parameter, any delayed or advanced operation of any cell compared to the rest of cells may deteriorate the output signal.

In this paper, an H6 cell-based multilevel converter is proposed, where the issue of the timing can be fixed as explained and investigated in the following.

II. PROPOSED MULTILEVEL TOPOLOGY

A dc-dc converters can be placed between each PV string and H-bridge, which ensures a decoupled control between the PV voltage and the H-bridge dc-link voltage. The dc-dc converter can be a boost, buck, or flyback converter [18]. However, this solution adds more passive elements, consequently, the hardware is sizable and more expensive. For this purpose, H6 bridge has been chosen to replace the H-bridge in each cell, in which the dc-link capacitor is replaced by a split dc-link capacitor, and only two active switches and two diodes are added. The overall schematic of the proposed multilevel converter for PV application, where n cell are considered, is illustrated in Fig. 1. The proposed concept consists of injecting power with less voltage from the shaded

cells without altering the PV voltage, and hence, the MPPT. The control of the proposed topology is divided into three parts, the grid injected current control, an independent MPP tracking in each cell, and H6 capacitors insertion and voltage control.

Each cell output voltage can be assessed as the following:

$$v_{Subi} = (S_{1i} - S_{2i}) \cdot (S_{5i}v_{C5i} + S_{6i}v_{C6i}) \quad i = 1, \dots, n \quad (1)$$

where S_{xi} is the xi semiconductor state (which could be either on or off), according to Fig. 1, i refers to the cell index and x denotes to the semiconductor number in that cell. v_{Subi} , v_{C5i} , and v_{C6i} are the output voltage, the voltage across the capacitor C_5 and the voltage across the capacitor C_6 of the i^{th} cell, respectively.

If the capacitors in each cell are balanced, the cell voltage can be expressed as:

$$v_{Subi} = (S_{1i} - S_{2i}) \cdot \left(\frac{S_{5i} + S_{6i}}{2} \right) \cdot v_{PV_i} \quad (2)$$

such as, v_{PV_i} is the voltage of the i^{th} PV array.

The dynamic behavior of each cell can be defined by the following differential equation:

$$C_{\{5,6\}i} \frac{dv_{C\{5,6\}i}}{dt} = (i_{PV_i} - (S_{1i} - S_{2i}) \cdot S_{\{5,6\}i} \cdot i_g) \quad (3)$$

Thus, according to Kirchhoff's voltage law, the dynamic behavior of the overall system can be determined as follows:

$$L_f \frac{di_g}{dt} = \sum_{i=1}^n \left((S_{1i} - S_{2i}) \cdot \left(\frac{S_{5i} + S_{6i}}{2} \right) \cdot v_{PV_i} \right) - r_f \cdot i_g - v_g \quad (4)$$

where v_g , i_g , L_f , and r_f are the grid voltage, the injected current to the grid, the filter inductance, and the filter stray resistor, respectively.

III. CONTROL STRUCTURE

In the literature, many controls have been proposed for the cascaded H-bridge. These controls are suitable for the case where the converter is used in rectifier mode or in inverter mode. Their merits are analyzed and investigated in [20]. The classical control, with one Proportional Integral (PI) controller for each cell voltage and one Proportional Resonant (PR) controller for the output current is adopted in this paper (see Fig. 2). This control strategy has proven to be the most efficient when using different voltages in the cells, which is the case here since these voltages will be determined by using separate MPP trackers [12], [19], [20].

As can be seen from Fig. 2, from $i=2$ to n , the cells voltages are the only controlled variables in the loops. The voltages are controlled through a PI controllers, which their outputs provide the modulation indexes. These PI controllers can be expressed as the following:

$$U_i^{peak} = K_{PV} \cdot (v_{PV_i} - v_{PV_i}^{ref}) + \frac{K_{Iv}}{s} (v_{PV_i} - v_{PV_i}^{ref}) \quad (5)$$

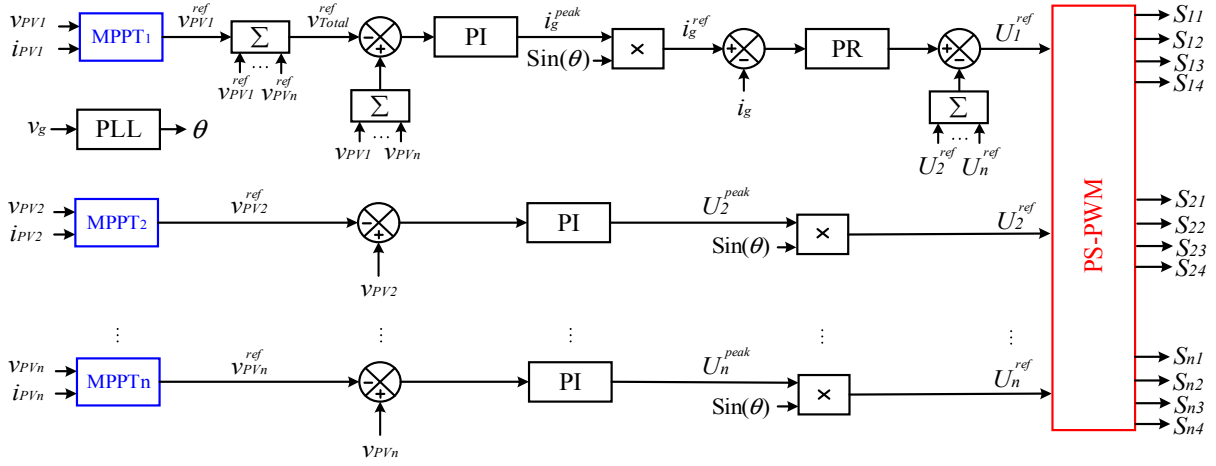


Fig. 2. Control structure of the cascaded H-bridge.

where K_{Pv} and K_{Iv} are the proportional and integral gains of the cell voltage loop, respectively, and U_i^{peak} is the modulation index of the i^{th} cell. In order to obtain the switching functions, these modulation indexes are multiplied by a normalized sinusoidal signal, that is synchronized with the grid voltage. The phase angle of that later is determined through a Phase Locked Loop (PLL).

In the first cell, one PI controller is designated to control the total voltage based on all the voltage references provided by the MPPTs. The output of this controller generates the grid peak current (i_g^{peak}), which is multiplied by a unitary sinusoidal signal, that is synchronized with the grid voltage. The total voltage regulator can be written as follows:

$$i_g^{peak} = K_{Pv} \cdot \left(\sum_{i=1}^n v_{PVi} - \sum_{i=1}^n v_{PVi}^{ref} \right) + \frac{K_{Iv}}{s} \left(\sum_{i=1}^n v_{PVi} - \sum_{i=1}^n v_{PVi}^{ref} \right) \quad (6)$$

such as K_{Pv} and K_{Iv} are the proportional and integral gains of the total voltage loop, respectively.

A PR controller caters the modulator reference that should be applied in order to obtain the grid current reference. The ideal PR controller is given by:

$$U_{Total}^{ref} = K_{Pi} \cdot (i_g - i_g^{ref}) + \frac{K_{Ri} (i_g - i_g^{ref}) s}{s^2 + \omega_g^2} \quad (7)$$

where K_{Pi} and K_{Ri} are the proportional and resonant gains of the grid current controller, and ω_g is the grid frequency. However, the ideal PR controller may cause instability problems due to the infinite resonant gain. The later problem can be solved by introducing a damping as follows:

$$U_{Total}^{ref} = K_{Pi} \cdot (i_g - i_g^{ref}) + \frac{2\omega_c K_{Ri} (i_g - i_g^{ref}) s}{s^2 + 2\omega_c s + \omega_g^2} \quad (8)$$

such as, ω_c represents the bandwidth around the grid frequency.

Since U_{Total}^{ref} represents the total switching function, the switching function of the first cell is assessed by subtracting

the sum of the rest of the switching functions from U_{Total}^{ref}

$$U_1^{ref} = U_{Total}^{ref} - \sum_{i=2}^n U_i^{ref} \quad (9)$$

The switching states of S_{xi} , where $i \in [1,4]$ (H-bridge switches), are generated from PS-PWM. Whereas, S_{xi} , where $i \in [5,6]$ (extra switches) are generated as shown in Fig. 3. In case, the irradiance is balanced among all cells, and the H-bridge is inserted, these two switches are both gated ON. If one of the cells is shaded, these switches are controlled differently. The switch corresponds to a higher capacitor voltage is gated ON when the H-bridge is inserted, i.e. if v_{C5i} is higher, then S_{5i} is gated ON when at the H-bridge is inserted, otherwise S_{6i} is gated ON. Note that, H_i in Fig. 3 determines whether the i^{th} cell is shaded or not, where it takes high logic value when the cell is shaded, and low logic value otherwise.

IV. SIMULATION RESULTS AND DISCUSSION

In this section, the proposed cascaded H6-inverter is designed and simulated in PLECS [21], as a 2.4-kW single-phase inverter. This inverter is designed to be fed from a PV strings, whose voltage ranges from 90 to 120V connected to a 4mF capacitors in each cell, whereas the grid rms voltage is 150 V. The PV strings are formed by a three series PV panels, whose specifications are as follows: $v_{OC}=38.9V$, $v_{MPP}=34.64V$, $i_{SC}=7.56A$, and $i_{MPP}=7.35A$. The grid fundamental and the switching frequencies have been set to 50Hz and 2.5kHz, respectively. The output inductor filter has been chosen to be 2mH. The MPPTs are the conventional Perturb and Observe (P&O) [22], and their frequency and

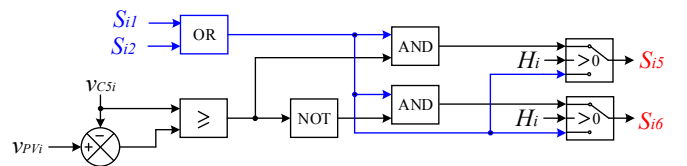


Fig. 3. Capacitors insertion in the partially shaded submodules.

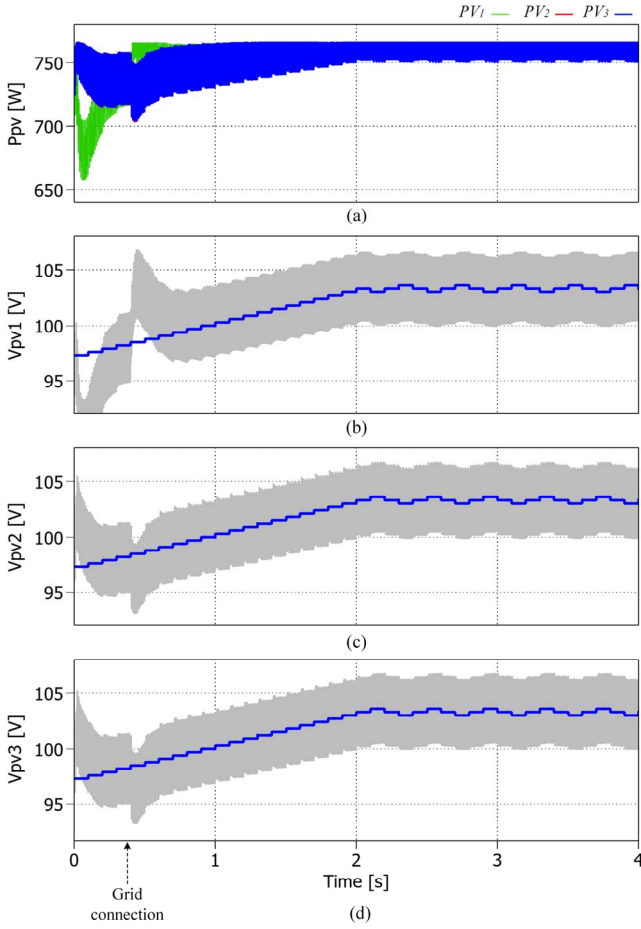


Fig. 4. Simulation results of the proposed topology showing the case of a balanced solar irradiance among the three cells, (a) the power drawn from the three strings, (b) the reference and measured voltage of the first PV string, (c) the reference and measured voltage of the second PV string, (d) the reference and measured voltage of the third PV string.

voltage step size have been set to 10Hz and 0.3V, respectively.

Fig. 4 shows the simulation results of the power extracted from the arrays and the cells voltages of the proposed topology when all the three cells are subjected to the standard test conditions (STC). The STC are 1 kW/m^2 irradiance and 25°C temperature. Note that, the lines of the power in cell one and two are not clear in the figure since they are congruent with the blue one. As can be seen from these two figures, the proposed topology provides a similar results to those reported in [12], whose are of the CHB in case of a balanced solar insolation.

A test that consists of two phases has been performed on the proposed topology. During the first phase, the switches S_{i5} and S_{i6} are turned ON simultaneously to simulate the operation of the CHB. After 4 seconds, the second phase of the test starts, and the semiconductor switches S_{i5} and S_{i6} begin their normal operation as explained earlier in section III. During both phases, the first and second cells were under the STC, whereas the third cell was subjected to 0.5 kW/m^2 irradiance. As can be seen from Fig. 6, the duty cycle of the third cell during the first phase has a peak value that is nearly half of the peaks of the duty cycles in cells one and two. As a result, the third cell is operating less than the rest of cells—during each switching period, the third cell starts after

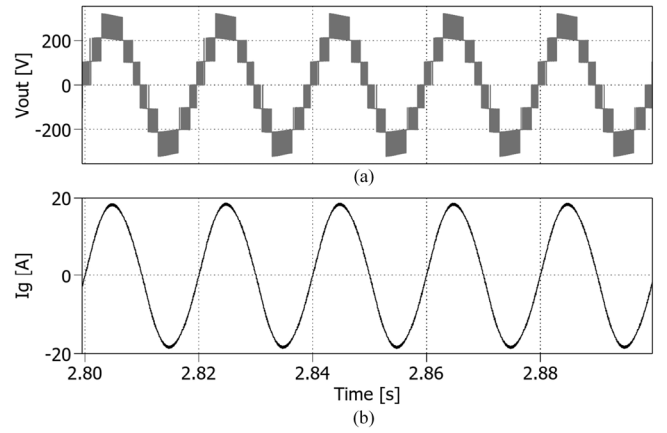


Fig. 5. (a) the output voltage, (b) the grid current, when the three PV strings of the proposed topology are under the stander test conditions.

a delay and stops in advance. Since in multilevel-cascaded converters all the cells form the same output signals (voltage and current), any advance or delay of any cell may deteriorate theses output signals.

The output voltage and the injected current of the seven level CHB (first phase) are shown in Fig. 7(a) and (b), respectively. One can note from Fig. 7(b), that the injected current has a ringing, which represents a high order harmonics due to the difference in duty cycles among the cells.

As can be seen from Fig. 6, at the starting of the second phase, where the converter begins to operate as a cascaded H6, the duty cycle of the first cell get affected since it is designated for the control of both the total and the first cell voltages. The duty cycle of the first cell settles down again after 0.2 second.

One can note from this figure, that the duty cycle of the shaded cell increases and ended up having nearly the same duty cycle in cell one and two after 0.2 second. As a consequence, and as it can be observed from Fig. 9(b), the current provided by the proposed topology does not present

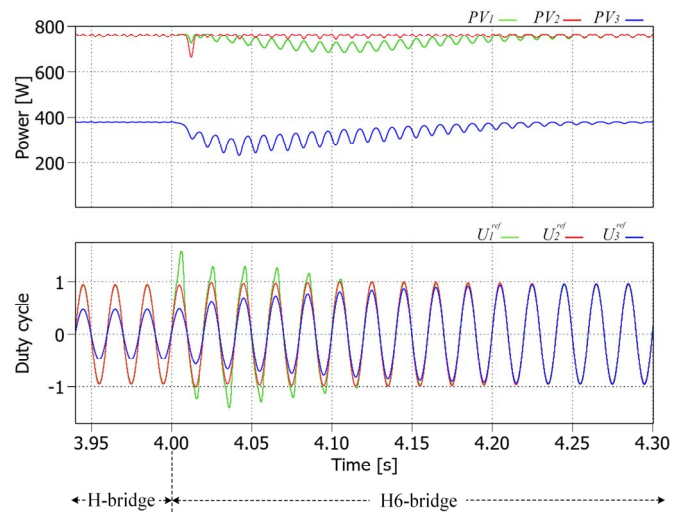


Fig. 6. The duty cycles of the three cells when the converter is operating first in H-bridge mode and then H6 mode. The first and second cell are under the STC, while the third one is under 500 W/m^2 .

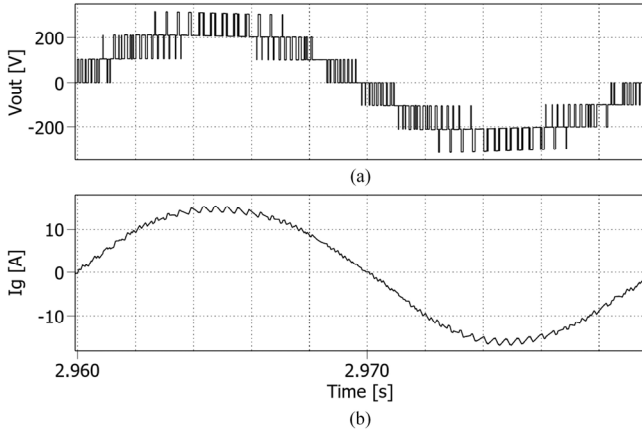


Fig. 7. Simulation results of the CHB when the first and second cell are subjected to 1KW/m^2 , whereas the irradiance of the third cell is 0.5KW/m^2 , (a) the output voltage, and (b) the injected current to the grid.

any ringing since the difference in duty cycles has been eliminated.

By inserting power with less voltage from the shaded cell, the instantaneous delivered power by the cell can be reduced. In order to keep tracking the MPP voltage and/or current in these conditions, the duty cycle has to be increased, which will keep the delivered power over a period of time at the MPP power.

The harmonic spectrums of the grid current in case of using CHB and the proposed topology are shown in Fig. 8. It can be seen from this figure, that in case of partial shading the CHB generates important harmonics located in the neighborhood of the switching frequency and its multiple ($2f_{sw}$). Contrastively, in the proposed topology these harmonics are significantly reduced. The effect of the different duty cycle values may also increase the low order harmonics. One can note from Fig. 8, that the fifth harmonic is also less in the proposed multilevel converter.

V. CONCLUSION

A solution to the distorted current in the multilevel-cascaded converters when the cells are subjected to a different irradiance levels has been proposed in this paper through a new topology. The proposed topology and its control have been explained. It has been verified in this paper, that the main cause of the current distortion in cascaded-multilevel converters in PV applications is the difference in duty cycle

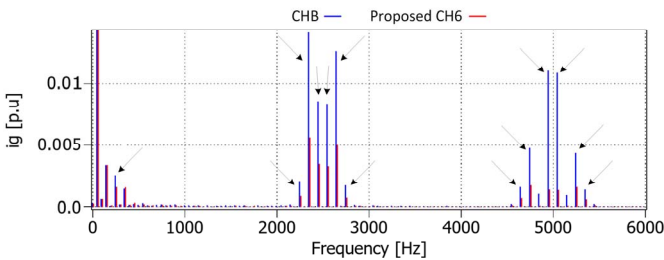


Fig. 8. Harmonic spectrums of the grid current in the CHB and the proposed topology.

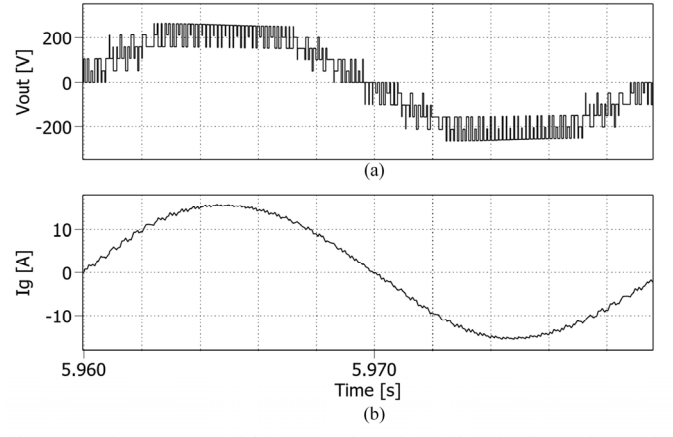


Fig. 9. Simulation results of the proposed topology when the first and second cell are subjected to 1KW/m^2 , whereas the irradiance of the third cell is 0.5KW/m^2 , (a) the output voltage, and (b) the injected current to the grid.

values. In the proposed topology, the duty cycle in the shaded cell can be increased to a similar level of the non-shaded cells duty cycles by decreasing the cell voltage seen by the output of the converter. The simulation results confirmed that the proposed converter provides a high quality current, while maintaining the MPP tracking in all cells.

VI. REFERENCES

- [1] R. Carbone, "Grid-connected photovoltaic systems with energy storage," in *Clean Electrical Power, 2009 International Conference on*, June 2009, pp. 760 -767.
- [2] A. Lashab, D. Sera, J. Martins and J. M. Guerrero, "Model Predictive-Based Direct Battery Control in PV Fed Quasi Z-Source Inverters," *2018 5th International Symposium on Environment-Friendly Energies and Applications (EFEA)*, Rome, 2018, pp. 1-6.
- [3] X. Guo *et al.*, "Leakage Current Suppression of Three-Phase Flying Capacitor PV Inverter With New Carrier Modulation and Logic Function," in *IEEE Trans. Power Electron.*, vol. 33, no. 3, pp. 2127-2135, March 2018.
- [4] S. Strache, R. Wunderlich and S. Heinen, "A Comprehensive, Quantitative Comparison of Inverter Architectures for Various PV Systems, PV Cells, and Irradiance Profiles," in *IEEE Trans. Sust. Energy*, vol. 5, no. 3, pp. 813-822, July 2014.
- [5] J. Schonberger, "A single phase multi-string PV inverter with minimal bus capacitance," *2009 13th European Conference on Power Electronics and Applications*, Barcelona, 2009, pp. 1-10.
- [6] C. Liao, W. Lin, Y. Chen and C. Chou, "A PV Micro-inverter With PV Current Decoupling Strategy," *IEEE Trans. on Power Electron.*, vol. 32, no. 8, pp. 6544-6557, Aug. 2017.
- [7] F. Rong, X. Gong and S. Huang, "A Novel Grid-Connected PV System Based on MMC to Get the Maximum Power Under Partial Shading Conditions," *IEEE Trans. Power Electron.*, vol. 32, no. 6, pp. 4320-4333, June 2017.
- [8] G. Farivar, B. Hredzak and V. G. Agelidis, "A DC-Side Sensorless Cascaded H-Bridge Multilevel Converter-Based Photovoltaic System," in *IEEE Trans. Indus. Electron.*, vol. 63, no. 7, pp. 4233-4241, July 2016.
- [9] Y. Yu, G. Konstantinou, B. Hredzak and V. G. Agelidis, "Power Balance of Cascaded H-Bridge Multilevel Converters for Large-Scale Photovoltaic Integration," in *IEEE Trans. Power Electron.*, vol. 31, no. 1, pp. 292-303, Jan. 2016.
- [10] Y. Yu, G. Konstantinou, B. Hredzak and V. G. Agelidis, "Operation of Cascaded H-Bridge Multilevel Converters for Large-Scale Photovoltaic Power Plants Under Bridge Failures," in *IEEE Trans. on Industrial Electronics*, vol. 62, no. 11, pp. 7228-7236, Nov. 2015.
- [11] A. Lashab, D. Sera, J. Martins and J. M. Guerrero, "Multilevel DC-Link Converter-Based Photovoltaic System with Integrated Energy

- Storage," *2018 5th International Symposium on Environment-Friendly Energies and Applications (EFEA)*, Rome, 2018, pp. 1-6. doi: 10.1109/EFEA.2018.8617110
- [12] E. Villanueva, P. Correa, J. Rodriguez and M. Pacas, "Control of a Single-Phase Cascaded H-Bridge Multilevel Inverter for Grid-Connected Photovoltaic Systems," in *IEEE Trans. Ind. Electron.*, vol. 56, no. 11, pp. 4399-4406, Nov. 2009.
- [13] J. I. Leon, S. Kouro, L. G. Franquelo, J. Rodriguez, and B. Wu, "The essential role and the continuous evolution of modulation techniques for voltage-source inverters in the past, present, and future power electronics," *IEEE Trans. Ind. Electron.*, vol. 63, no. 5, pp. 2688-2701, May 2016.
- [14] H. D. Tafti, A. I. Maswood, G. Konstantinou, C. D. Townsend, P. Acuna, and J. Pou, "Flexible Control of Photovoltaic Grid-Connected Cascaded H-Bridge Converters during Unbalanced Voltage Sags," *IEEE Trans. Ind. Electron.*, vol. 65, no. 8, pp. 6229-6238, 2018.
- [15] A. Marquez, J. I. Leon, S. Vazquez, R. Portillo, L. G. Franquelo, E. Freire, and S. Kouro, "Variable-angle phase-shifted pwm for multilevel three-cell cascaded h-bridge converters," *IEEE Trans. Ind. Electron.*, vol. 64, no. 5, pp. 3619-3628, May 2017.
- [16] A. Marquez, J. I. Leon, S. Vazquez, L. G. Franquelo, and S. Kouro, "Operation of an hybrid PV-battery system with improved harmonic performance," *IECON 2017 - 43rd Annu. Conf. IEEE Ind. Electron. Soc.*, pp. 4272-4277, 2017.
- [17] B. Xiao, L. Hang, J. Mei, C. Riley, L. M. Tolbert and B. Ozpineci, "Modular Cascaded H-Bridge Multilevel PV Inverter With Distributed MPPT for Grid-Connected Applications," in *IEEE Transactions on Industry Applications*, vol. 51, no. 2, pp. 1722-1731, March-April 2015.
- [18] H. Snani, M. Amarouayache, A. Bouzid, A. Lashab and H. Bounechba, "A study of dynamic behaviour performance of DC/DC boost converter used in the photovoltaic system," *2015 IEEE 15th International Conference on Environment and Electrical Engineering (EEEIC)*, Rome, 2015, pp. 1966-1971.
- [19] A. Lashab, D. Sera, J. Martins and J. M. Guerrero, "Multilevel DC-Link Converter-Based Photovoltaic System with Integrated Energy Storage," *2018 5th International Symposium on Environment-Friendly Energies and Applications (EFEA)*, Rome, 2018, pp. 1-6. doi: 10.1109/EFEA.2018.8617110
- [20] A. Dell'Aquila, M. Liserre, V. Monopoli, and P. Rotondo, "Overview of pi-based solutions for the control of DC buses of a single-phase H-bridge multilevel active rectifier," *IEEE Trans. Ind. Appl.*, vol. 44, no. 3, pp. 857-866, May/Jun. 2008.
- [21] K. Memar, P. Moamaei and R. Ahmadi, "Developing a hierarchical modular PV array model using PLECS block-set in MATLAB," *2015 IEEE Power and Energy Conference at Illinois (PECI)*, Champaign, IL, 2015, pp. 1-5.
- [22] A. Lashab, D. Sera, J. M. Guerrero, L. Mathe and A. Bouzid, "Discrete Model-Predictive-Control-Based Maximum Power Point Tracking for PV Systems: Overview and Evaluation," *IEEE Trans. Power Electron.*, vol. 33, no. 8, pp. 7273-7287, Aug. 2018.